Polymer Journal (2015) 47, 679–685

www.nature.com/pj

ORIGINAL ARTICLE

Translational diffusion coefficient of wormlike regular three-arm stars

Daichi Ida

Effects of chain stiffness on the translational diffusion coefficient D or (effective) hydrodynamic radius R_H ($\propto D^{-1}$) are examined theoretically for the regular three-arm star polymers on the basis of the Kratky–Porod (KP) wormlike chain model. The ratio g_H of R_H of the regular KP three-arm star touched-bead model to that of the KP linear one, both having the same (reduced) total contour length L and (reduced) bead diameter d_b, is numerically evaluated on the basis of the Kirkwood formula and/or the Kirkwood–Riseman (KR) hydrodynamic equation. From an examination of the behavior of the Kirkwood value $g_H^{(K)}$ and the KR one $g_H^{(KR)}$ of g_H as a function of L and d_b, it is found that both of $g_H^{(K)}$ and $g_H^{(KR)}$ are insensitive to change in L irrespective of the value of d_b and that $g_H^{(KR)}$ is slightly larger than $g_H^{(K)}$ in the ranges of L and d_b investigated. An empirical interpolation formula is constructed for $g_H^{(K)}$, which reproduces the asymptotic values $\sqrt{3}/(2\sqrt{2}-1)$ (=0.947) in the random-coil limit and 1 in the thin-rod limit.
Polymer Journal (2015) **47,** 679–685; doi:10.1038/pj.2015.44; published online 17 June 2015

INTRODUCTION

We have made theoretical and/or computational studies of the intrinsic viscosity $[\eta]$[1,2] and second virial coefficient A_2[3] of the semiflexible regular three-arm stars. The quantities $[\eta]$ and A_2 are measures of the average chain dimension as well as the mean-square radius of gyration $\langle S^2 \rangle$, although A_2 is related to the chain dimension only in good solvents or perturbed state. The ratio of g_η of $[\eta]$ of an unperturbed regular three-arm star chain to that of the corresponding unperturbed linear one, both having the same molecular weight and chain stiffness, has been shown to become remarkably smaller than the random-coil limiting value as the chains become stiffer, as in the case of the ratio g_S of $\langle S^2 \rangle$ of the former chain to that of the latter.[4] Further, for practical purposes, an empirical interpolation formula for g_η has been constructed. However, the ratio g_{A_2} of A_2 of a perturbed regular three-arm star chain to that of the corresponding perturbed linear one has been shown to be rather insensitive to change in chain stiffness.

The (effective) hydrodynamic radius R_H is another measure of the chain dimension and is defined from the translational diffusion coefficient D as follows:

$$R_H = k_B T/6\pi\eta_0 D, \tag{1}$$

where k_B is the Boltzmann constant, T is the absolute temperature and η_0 is the viscosity coefficient of the solvent. It is then interesting and necessary to examine the effects of chain stiffness on the ratio g_H of R_H of the regular three-arm star chain to that of the corresponding linear one. In this paper, we evaluate g_H of the semiflexible regular three-arm star polymer on the basis of the Kratky–Porod (KP) chain without excluded volume as in the case of the previous study of g_η,[2] and then, we construct an interpolation formula for g_H for practical purposes.

For an evaluation of D for both of the KP regular three-arm star and linear chains, we adopt the touched-bead hydrodynamic model as in the case of the previous study of $[\eta]$.[2] And also, we use the Kirkwood formula[5–7] as in the case of the linear helical wormlike touched-bead model[8,9] including the KP chain as a special case. On the basis of the Kirkwood formula, for unperturbed linear chains in the random-coil limit, there holds the asymptotic relation:

$$D = 0.196 k_B T/\eta_0 \langle R^2 \rangle^{1/2} \qquad \text{(linear, Kirkwood)}, \tag{2}$$

where $\langle R^2 \rangle$ is the mean-square end-to-end distance of the chains. On the other hand, if D is evaluated from the Kirkwood–Riseman (KR) hydrodynamic equation in the scheme of preaveraged hydrodynamic interaction (HI),[7,10] we have another asymptotic relation given by

$$D = 0.192 k_B T/\eta_0 \langle R^2 \rangle^{1/2} \qquad \text{(linear, KR)}. \tag{3}$$

Note that the correct numerical factor 0.192 of Equation (3) was obtained by Kurata and Yamakawa[11] instead of the original approximate one 0.196 obtained in the so-called KR approximation for D.[7,10] We also note that the Zimm theory[12] on the basis of the unperturbed (dynamic) Gaussian spring-bead model in the scheme of preaveraged HI gives the latter relation. The difference between the prefactor of the right-hand side of Equation (2) and that of Equation (3) is arising from the fact that the Kirkwood and KR (or Zimm) values of D correspond to the translational diffusion of the center of mass of the polymer chain and that of the Zimm center of resistance[7,12] as defined as the point where the translational motion of the entire chain becomes independent of the internal (segmental) motions in the scheme of preaveraged HI, respectively.[8,13,14] This may be expected to

Department of Polymer Chemistry, Kyoto University, Kyoto, Japan
Correspondence: Dr D Ida, Department of Polymer Chemistry, Kyoto University, Katsura, Kyoto 615–8510, Japan.
E-mail: ida@molsci.polym.kyoto-u.ac.jp
Received 23 March 2015; revised 17 April 2015; accepted 1 May 2015; published online 17 June 2015

be the case with the star polymers. We then also evaluate D (or R_H) and g_H for the KP regular three-arm star chain following the KR procedure and examine difference between the Kirkwood and KR values of R_H and g_H. This is another purpose of this paper.

MATERIALS AND METHODS

The model used in this study is the same as that used in the previous one,[2] that is, a regular three-arm star touched-bead model composed of $3m+1$ identical spherical beads of (hydrodynamic) diameter d_b whose centers are located on the KP regular three-arm star chain contour (see Figure 1 in Ref. 2). For convenience, the three arms are designated the first, second and third ones, and the m beads on the ith ($i=1$, 2, 3) arm are numbered $(i-1)m+1$, $(i-1)m+2$, …im from the branch point (center) to the terminal end, with the center bead numbered 0. The angle between each pair of the unit vectors tangent to the KP contours at the branch point is fixed to be 120°, so that the three vectors are on the same plane. The linear touched-bead model, the counterpart of the above star one, is the KP touched-bead model composed of $n+1$ identical beads of diameter d_b whose centers are located on the KP linear chain contour. We set $n+1$ equal to $3m+1$, so that $n=3m$. The $n+1$ beads are numbered 0, 1, 2, …, n from one end to the other. For both the star and linear touched-bead models, the contour distance between the two adjacent beads is set equal to d_b. In what follows, all lengths are measured in units of the stiffness parameter λ^{-1} of the KP chain unless otherwise specified.

Kirkwood formula

The Kirkwood formula for D of the chain composed of $n+1$ beads may be given by[5–7]

$$D=\frac{k_BT}{(n+1)\zeta}\left[1+\frac{\zeta}{6\pi\eta_0(n+1)}\sum_{i=0}^{n}\sum_{\substack{j=0\\ i\neq j}}^{n}\left\langle R_{ij}^{-1}\right\rangle\right], \tag{4}$$

where $\zeta=3\pi\eta_0 d_b$ is the translational friction coefficient of bead and $\left\langle R_{ij}{}^{-1}\right\rangle$ is the mean reciprocal of the distance between the centers of the ith and jth beads.

For the $[(i-1)m+k]$th and $[(j-1)m+l]$th beads ($i, j=1, 2, 3$; $k, l=1, 2, \ldots, m$) of the KP regular three-arm star chain, that is, the kth bead on the ith arm and the lth bead on the jth arm, respectively, $\left\langle R_{[(i-1)m+k][(j-1)m+l]}{}^{-1}\right\rangle$ may be given by

$$\left\langle R_{[(i-1)m+k][(j-1)m+l]}{}^{-1}\right\rangle=\left\langle R^{-1}\left(t_k^{(i)},t_l^{(j)}\right)\right\rangle \tag{5}$$

with $t_k^{(i)}$ denoting the contour distance from the branch point to the contour point on the ith arm where the center of the $[(i-1)m+k]$th bead locates on, so that

$$t_k^{(i)}=kd_b. \tag{6}$$

The theoretical expression for $\left\langle R^{-1}\left(t_k^{(i)},t_l^{(j)}\right)\right\rangle$ has been obtained in the previous paper.[2] Here we give only the results with a brief description. For the KP regular three-arm star chain under the consideration, $\left\langle R^{-1}\left(t_k^{(i)},t_l^{(j)}\right)\right\rangle$ may be given by

$$\begin{aligned}\left\langle R^{-1}\left(t_k^{(i)},t_l^{(j)}\right)\right\rangle&=\left\langle R^{-1}\left(t_k^{(i)},t_l^{(j)},120^\circ\right)\right\rangle \quad \text{for } i\neq j\\ &=\left\langle R^{-1}\left(\left|t_k^{(i)}-t_l^{(i)}\right|,0,120^\circ\right)\right\rangle \quad \text{for } i=j,\end{aligned} \tag{7}$$

where $\langle R^{-1}(t_1,t_2,120^\circ)\rangle$ is the mean reciprocal of the end-to-end distance of the (unperturbed) once-broken KP chain of total contour length t_1+t_2 such that two KP subchains 1 and 2 of contour lengths t_1 and t_2, respectively, are connected with a bending angle $\theta=120°$ (see Figure 2 in Ref. 2). We note that $\langle R^{-1}(t,0,120^\circ)\rangle$ and/or $\langle R^{-1}(0,t,120^\circ)\rangle$ represent the mean reciprocal of the end-to-end distance of the KP linear chain of contour length t. The interpolation formula for $\langle R^{-1}(t_1,t_2,120^\circ)\rangle$ may be given by

$$\begin{aligned}\langle R^{-1}(t_1,t_2,120^\circ)\rangle=&\langle R^2\rangle^{-1/2}\left[1+5\langle R^2\rangle^{11/2}\right]^{-1}\\ &\times\left[f_{\epsilon\epsilon}(t_1,t_2,120^\circ)+0.045\langle R^2\rangle^{3/2}\right.\\ &+0.40t_1t_2(t_1+t_2)e^{-t_1t_2}\\ &\left.+5\langle R^2\rangle^{11/2}f_{DD\epsilon}(t_1,t_2,120^\circ)\right],\end{aligned} \tag{8}$$

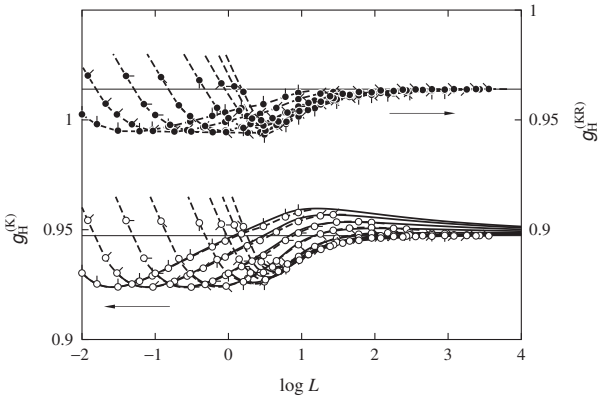

Figure 1 Plots of $g_H^{(K)}(L,d_b)$ and $g_H^{(KR)}(L,d_b)$ against log L. The open and closed circles represent $g_H^{(K)}$ and $g_H^{(KR)}$, respectively, for $d_b=0.001$ (pip up), 0.003 (pip right-up), 0.01 (pip right), 0.03 (pip right-down), 0.1 (pip down), 0.2 (pip left-down), 0.3 (pip left) and 0.4 (pip left-up). The dashed curves connect smoothly the theoretical values at constant d_b. The lower and upper horizontal lines represent the random-coil limiting values $\sqrt{3}/\left(2\sqrt{2}-1\right)$ (=0.947) of $g_H^{(K)}$ and 0.96_4 of $g_H^{(KR)}$, respectively. The solid curves represent the values calculated from the interpolation formula for $g_H^{(K)}$ (see the text).

where

$$f_{\epsilon\epsilon}(t_1,t_2,\theta)=1+\frac{3}{8}\left(\frac{\langle R^4\rangle}{\langle R^2\rangle^2}-1\right), \tag{9}$$

$$f_{DD\epsilon}(t_1,t_2,120^\circ)=\left(\frac{6}{\pi}\right)^{1/2}\left[1-\frac{11}{40\langle R^2\rangle}+\frac{431}{4480\langle R^2\rangle^2}+\frac{C(t_1,t_2)}{\langle R^2\rangle^2}\right], \tag{10}$$

and $C(t_1,t_2)$ is given by

$$C(t_1,t_2)=\frac{108\bar{t}^2+77\bar{t}^4}{640\left(1+\bar{t}^4\right)} \tag{11}$$

with

$$\bar{t}^2=\left(t_1^{-2}+t_2^{-2}\right)^{-1}. \tag{12}$$

In Equations (8)–(10) $\langle R^2\rangle=\langle R^2(t_1,t_2,\theta)\rangle$ and $\langle R^4\rangle=\langle R^4(t_1,t_2,\theta)\rangle$ are the second and fourth moments, respectively, of the end-to-end distance of the once-broken KP chain that are given by

$$\begin{aligned}\left\langle R^2(t_1,t_2,\theta)\right\rangle=&\,t_1+t_2-\frac{1}{2}\left[1-e^{-2(t_1+t_2)}\right]\\ &-\frac{1}{2}\left(1-e^{-2t_1}\right)\left(1-e^{-2t_2}\right)(1+\cos\theta),\end{aligned} \tag{13}$$

$$\begin{aligned}&\left\langle R^4(t_1,t_2,\theta)\right\rangle\\ &=\frac{5}{3}(t_1+t_2)^2-(t_1+t_2)\left[\frac{26}{9}+e^{-2(t_1+t_2)}\right]\\ &+2\left[1-e^{-2(t_1+t_2)}\right]-\frac{1}{54}\left[1-e^{-6(t_1+t_2)}\right]\\ &-\left\{\left(1-e^{-2t_1}\right)\left[\frac{5}{3}t_2+t_2e^{-2t_2}-\frac{3}{2}\left(1-e^{-2t_2}\right)+\frac{1}{18}\left(1-e^{-6t_2}\right)\right]\right.\\ &\left.+\left(1-e^{-2t_1}\right)\left[\frac{5}{3}t_1+t_1e^{-2t_1}-\frac{3}{2}\left(1-e^{-2t_1}\right)+\frac{1}{18}\left(1-e^{-6t_1}\right)\right]\right\}\\ &\times(1+\cos\theta)-\frac{1}{4}\left[\left(1-e^{-2t_1}\right)-\frac{1}{3}\left(1-e^{-6t_1}\right)\right]\\ &\times\left[\left(1-e^{-2t_2}\right)-\frac{1}{3}\left(1-e^{-6t_2}\right)\right](1-\cos^2\theta).\end{aligned} \tag{14}$$

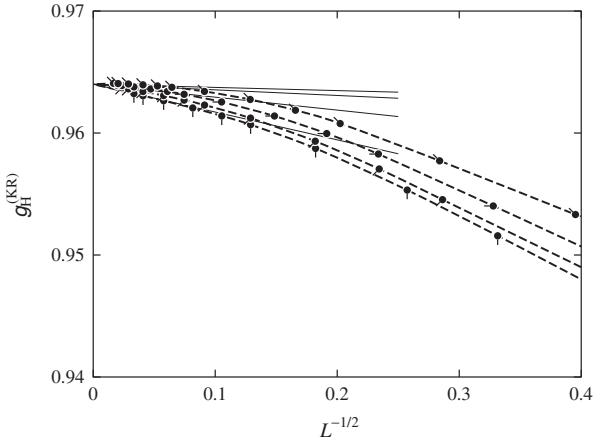

Figure 2 Plots of $g_H^{(KR)}$ against $L^{-1/2}$. All the symbols have the same meaning as those in Figure 1. The dashed curves connect smoothly the theoretical values at constant d_b and the solid lines indicate the respective initial tangents.

We note that the expression for $\langle R^2(t_1,t_2,\theta)\rangle$ given by Equation (13) was first derived by Mansfield–Stockmayer.[4] In the rod limit, Equation (8) reduces to

$$\left\langle R^{-1}(t_1,t_2,120^\circ)\right\rangle = \left(t_1^2+t_2^2+t_1t_2\right)^{-1/2} \text{ (rod limit)}. \tag{15}$$

For later convenience, D obtained from Equation (2) is designated $D^{(K)}$ hereafter.

Kirkwood–Riseman equation

On the basis of the KR hydrodynamic equation in the scheme of preaveraged HI,[7,10] D of the chain composed of n+1 beads may be written as follows:

$$D = k_BT/\zeta\sum_{i=0}^{n}\psi_i, \tag{16}$$

where ψ_i is the solution of the following linear simultaneous equations:

$$\psi_i = 1-\frac{\zeta}{6\pi\eta_0}\sum_{\substack{j=0\\ \neq i}}^{n}\left\langle R_{ij}^{-1}\right\rangle\psi_j. \tag{17}$$

The expression for $\langle R_{ij}^{-1}\rangle$ has already been given by Equation (5) with Equations (7)–(14). We note that if we assume $\psi_i=(n+1)^{-1}\psi$, that is, the average force exerted on the solvent of the ith bead equal to the average total force of the entire chain divided by n+1, for all i, Equations (16) and (17) may reduce to Equation (4). We also note that this assumption is equivalent to the KR approximation for D mentioned in the Introduction section. For later convenience, D obtained from Equations (16) and (17) is designated $D^{(KR)}$ hereafter.

RESULTS AND DISCUSSION

We have calculated the Kirkwood value $D^{(K)}$ and the KR one $D^{(KR)}$ of the translational diffusion coefficient D from Equation (4) and from Equation (16) with the numerical solution ψ_i of the linear simultaneous equations (17), respectively, for both the KP regular three-arm star and linear touched-bead models, in the ranges of the total number n+1 of bonds from 4 to 9001 and of the bead diameter d_b from 0.001 to 0.4. Note that the total contour length L of the chain is equal to $(n+1)d_b$, as already mentioned in the Materials and methods. In Equations (4) and (17), $\langle R_{ij}^{-1}\rangle$ is given by Equation (5) with Equations (7)–(14). On the basis of the values of $D^{(K)}$ and $D^{(KR)}$ for the star and linear chains having the same L and d_b so obtained along with Equation (1), we evaluate the Kirkwood value $g_H^{(K)}$ and the KR one $g_H^{(KR)}$ of the ratio g_H as functions of L and d_b defined by

$$g_H^{(K)}(L,d_b) = \frac{R_H^{(K)}(\text{star})}{R_H^{(K)}(\text{linear})} = \frac{D^{(K)}(\text{linear})}{D^{(K)}(\text{star})} \tag{18}$$

and

$$g_H^{(KR)}(L,d_b) = \frac{R_H^{(KR)}(\text{star})}{R_H^{(KR)}(\text{linear})} = \frac{D^{(KR)}(\text{linear})}{D^{(KR)}(\text{star})}, \tag{19}$$

respectively.

In the following subsections, we first examine the behavior of $g_H^{(K)}$ and $g_H^{(KR)}$ as functions of L and d_b and compare the theoretical values of the two ratios. Then we construct an interpolation formula for $g_H^{(K)}$.

Comparison between $g_H^{(K)}$ and $g_H^{(KR)}$

Figure 1 shows plots of g_H against the logarithm of L. The open and closed circles represent the theoretical values of $g_H^{(K)}$ and $g_H^{(KR)}$, respectively, for $d_b=0.001$ (pip up), 0.003 (pip right-up), 0.01 (pip right), 0.03 (pip right-down), 0.1 (pip down), 0.2 (pip left-down), 0.3 (pip left) and 0.4 (pip left-up); the dashed curves connecting smoothly the respective theoretical values at constant d_b. The solid curves represent the values calculated from an interpolation formula for $g_H^{(K)}$, as discussed later.

In the case of $g_H^{(K)}$, the asymptotic value in the random-coil limit, that is, the limit $L\to\infty$ (in units of λ^{-1}) may be given by

$$\lim_{L\to\infty} g_H^{(K)}(L,d_b) = \sqrt{3}/\left(2\sqrt{2}-1\right) = 0.947 \text{ (random coil)}, \tag{20}$$

which may be calculated from the relation $g_H^{(K)} = \left[\left(\sqrt{2}-1\right)f^{1/2}+\left(2-\sqrt{2}\right)f^{-1/2}\right]^{-1}$ obtained for the Gaussian regular f-arm stars by Kurata and Fukatsu[15] and by Stockmayer and Fixman[16] (the latter authors using the KR approximation for D). The asymptotic value is represented by the lower horizontal line. As L is decreased, $g_H^{(K)}$ first increases from the random-coil limiting value and then decreases and exhibits a minimum after passing through a maximum, in the range of d_b investigated except for $d_b=0.4$. The behavior of $g_H^{(K)}$ depends also on d_b. It should be noted that the difference between the maximum and minimum of $g_H^{(K)}$ is rather small (4% at most).

As for $g_H^{(KR)}$, its values are slightly (3% at most) larger than those of $g_H^{(K)}$ and exhibit no appreciable maximum in contrast to the case of $g_H^{(K)}$, in the ranges of L and d_b investigated. We have evaluated the random-coil limiting value of $g_H^{(KR)}(L,d_b)$ from the numerical theoretical values with large d_b. Figure 2 shows plots of $g_H^{(KR)}$ against $L^{-1/2}$ for $d_b=0.1$, 0.2, 0.3 and 0.4. All the symbols have the same meaning as those in Figure 1. The dashed curves connect smoothly the theoretical values at constant d_b and solid lines indicate the respective initial tangents. It is seen that as $L^{-1/2}$ is decreased to 0 ($L\to\infty$), $g_H^{(KR)}$ approaches a constant value irrespective of the value of d_b. On the basis of such numerical results, it may be concluded that

$$\lim_{L\to\infty} g_H^{(KR)}(L,d_b) = 0.96_4 \text{ (random coil)}. \tag{21}$$

Note that the values of $g_H^{(KR)}$ for smaller d_b have been omitted in Figure 2, since we cannot make $L^{-1/2}$ ($=[(n+1)d_b]^{-1/2}$) small enough to evaluate $g_H^{(KR)}$ at $L^{-1/2}=0$. We also note that the asymptotic value so obtained is consistent with an available theoretical value of 0.96 obtained by Irurzun[17] for the Gaussian regular three-arm star chain without excluded volume on the basis of the KR equation. In Figure 1, the upper horizontal line represents the asymptotic value 0.96_4.

This asymptotic value is 1.8% larger than that of $g_H^{(K)}$ given by Equation (20).

For an examination the difference between $g_H^{(K)}$ and $g_H^{(KR)}$, it is useful to derive the asymptotic relations between R_H and $\langle S^2\rangle^{1/2}$ in the random-coil limit for both of the regular three-arm star and linear chains. From Equations (2) and (3), using the asymptotic relation $\langle R^2\rangle = 6\langle S^2\rangle$ for the linear chain[7] in this limit along with Equation (1), we may obtain

$$R_H^{(K)} = 0.663\langle S^2\rangle^{1/2} \quad \text{(random coil, linear)}, \tag{22}$$

$$R_H^{(KR)} = 0.677\langle S^2\rangle^{1/2} \quad \text{(random coil, linear)}. \tag{23}$$

As for the regular three-arm star chain in the random-coil limit, from Equations (18)–(23) using the asymptotic value 7/9 of g_S,[18] we then obtain the relations

$$R_H^{(K)} = 0.712\langle S^2\rangle^{1/2} \quad \text{(random coil, star)}, \tag{24}$$

and

$$R_H^{(KR)} = 0.740\langle S^2\rangle^{1/2} \quad \text{(random coil, star)}. \tag{25}$$

It is seen that for the regular three-arm star chain $R_H^{(KR)}$ is 3.8% larger than $R_H^{(K)}$, while for the linear chain the former value is 2.1% larger than the latter.

Further we give the asymptotic forms of $g_H^{(K)}$ and $g_H^{(KR)}$ in the thin-rod limit, that is, the limit of $L \to 0$ (in units of λ^{-1}) and $L/d_b \to \infty$. In this limit, $D^{(K)}$ for the regular three-arm star chain may be written in the form (see Appendix):

$$\lim_{\substack{L\to 0\\ L/d_b\to\infty}} D^{(K)} = \frac{k_B T \ln(L/d_b)}{3\pi\eta_0 L} \quad \text{(thin rod limit, star)}. \tag{26}$$

As for the linear chain, we have[7]

$$\lim_{\substack{L\to 0\\ L/d_b\to\infty}} D^{(K)} = \frac{k_B T \ln(L/d_b)}{3\pi\eta_0 L} \quad \text{(thin rod limit, linear)}. \tag{27}$$

We note that Equation (27) may be obtained directly from Equation (4) with Equations (5), (7), and (15) along with the relation $L = (n+1)d_b$. In the rod limit, $g_H^{(K)}$ should be a function only of L/d_b, that is,

$$\lim_{L\to 0} g_H^{(K)}(L, d_b) = g_{H,0}^{(K)}(L/d_b) \quad \text{(rod limit)}. \tag{28}$$

From Equation (18) with Equations (26)–(28) we have

$$\lim_{L/d_b\to\infty} g_{H,0}^{(K)}(L/d_b) = 1 \quad \text{(thin rod limit)}. \tag{29}$$

On the other hand, $D^{(KR)}$ for the regular three-arm star chain (see Appendix) and that for the linear one[19] in the thin-rod limit may be written in the forms:

$$\lim_{\substack{L\to 0\\ L/d_b\to\infty}} D^{(KR)} = \frac{k_B T \ln(L/d_b)}{3\pi\eta_0 L} \quad \text{(thin rod limit, star)} \tag{30}$$

and

$$\lim_{\substack{L\to 0\\ L/d_b\to\infty}} D^{(KR)} = \frac{k_B T \ln(L/d_b)}{3\pi\eta_0 L} \quad \text{(thin rod limit, linear)}, \tag{31}$$

respectively. In the rod limit, $g_H^{(KR)}$ should also be a function only of L/d_b, that is,

$$\lim_{L\to 0} g_H^{(KR)}(L, d_b) = g_{H,0}^{(KR)}(L/d_b) \quad \text{(rod limit)}. \tag{32}$$

From Equation (19) with Equations (30)–(32) we have

$$\lim_{L/d_b\to\infty} g_{H,0}^{(KR)}(L/d_b) = 1 \quad \text{(thin rod limit)}. \tag{33}$$

All of these equations for $D^{(KR)}$ and $g_H^{(KR)}$ have the same forms as the corresponding ones for $D^{(K)}$ and $g_H^{(K)}$ given by Equations (26),(27) and (29).

Such salient results given by Equations (29) or (33), that the translational diffusion coefficient of the regular three-arm star chain becomes identical with that of the corresponding linear chain in the thin-rod limit may be regarded as indicating the defect of the Kirkwood formula or that of the scheme of preaveraged HI as in the case of rigid rings.[7,8,20–24]

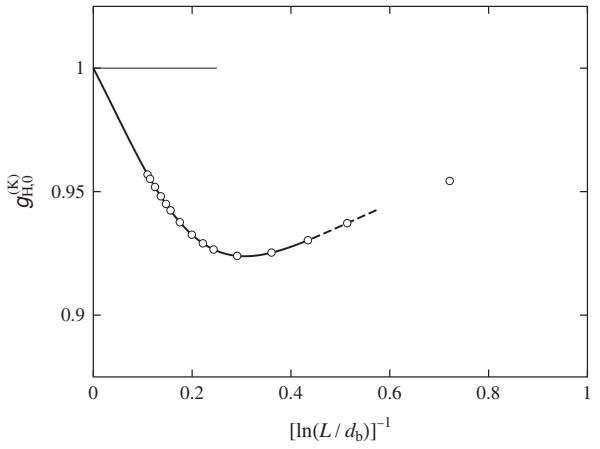

Figure 3 Plots of $g_{H,0}^{(K)}(L/d_b)$ against $[\ln(L/d_b)]^{-1}$. The open circles represent the theoretical values. The horizontal line segment represent the asymptotic value 1 in the limit of $[\ln(L/d_b)]^{-1} \to 0$ ($L/d_b \to \infty$). The curve represents the values of the interpolation formula, the solid part indicating the range of $L/d_b \gtrsim 10$ (see the text).

Interpolation formula for $g_H^{(K)}$

Now we are in a position to construct an interpolation formula for $g_H^{(K)}$ on the basis of the numerical theoretical values of $g_H^{(K)}(L,d_b)$ as already shown in Figure 1 along with the asymptotic relations given by Equations (20) and (29) in the random coil and thin-rod limits, respectively.

We have evaluated $g_{H,0}^{(K)}(L/d_b)$ numerically in the same manner as $g_H^{(K)}(L,d_b)$ mentioned above using the expression $\langle R_{ij}^{-1}\rangle$ given by Equations (5),(7) and (15) in place of that for the KP chain. Figure 3 shows plots of $g_{H,0}^{(K)}$ against $[\ln(L/d_b)]^{-1}$. The open circles represent the values so obtained. As $[\ln(L/d_b)]^{-1}$ is decreased (L/d_b is increased), $g_{H,0}^{(K)}$ first decreases and then increases to the asymptotic value 1 after passing through a minimum. For later convenience, we have constructed an interpolation formula for $g_{H,0}^{(K)}(L/d_b)$ in the range of $L/d_b \gtrsim 10$, which is given by

$$g_{H,0}^{(K)}(x) = \frac{1 - 1.84723(\ln\ x)^{-1} + 9.01492(\ln\ x)^{-2}}{1 - 1.46180(\ln\ x)^{-1} + 8.88140(\ln\ x)^{-2}} \quad \text{for } x \gtrsim 10. \tag{34}$$

In Figure 3, the curve represents the values calculated from Equation (34) with $x = L/d_b$. The error in the value of $g_{H,0}^{(K)}(L/d_b)$ in the range of $L/d_b \gtrsim 10$ (solid part) does not exceed 0.1%.

Next, we consider the ratio $g_H^{(K)}/g_{H,0}^{(K)}$. Figure 4 shows plots of $g_H^{(K)}(L,d_b)/g_{H,0}^{(K)}(L/d_b)$ against the logarithm of L, where $g_H^{(K)}/g_{H,0}^{(K)}$ has

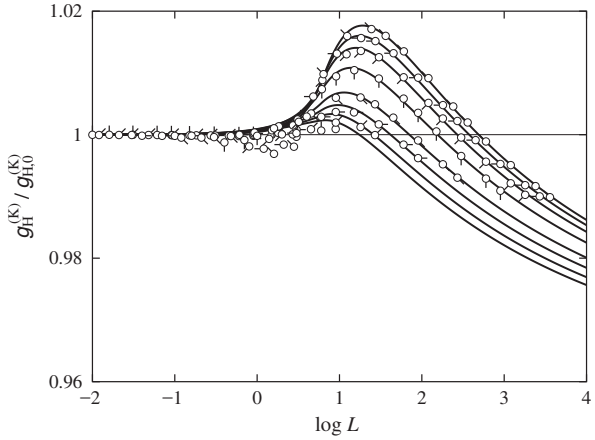

Figure 4 Plots of $g_H^{(K)}(L, d_b)/g_{H,0}^{(K)}(L/d_b)$ against log L. All the symbols have the same meaning as those in Figure 1. The solid curves represent the values of the interpolation formula with the corresponding values of d_b (see the text).

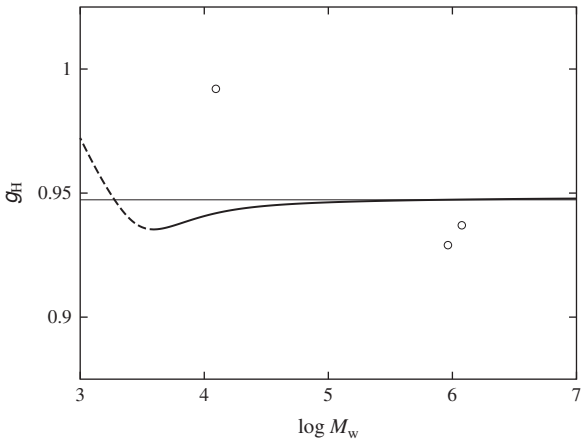

Figure 5 Plots of g_H against the logarithm of M_w for regular three-arm star polystyrenes in cyclohexane at 34.5 °C (Θ). The open circles represent the experimental data obtained by Huber *et al.*[25] The curve represents the corresponding KP theory values, the solid part indicating the range of $L/d_b \gtrsim 10$ (see text).

been evaluated by dividing the $g_H^{(K)}$ values shown in Figure 1 by the $g_{H,0}^{(K)}$ values calculated from Equation (34) with $x = L/d_b$. All the symbols in Figure 4 have the same meaning as those in Figure 1. It is seen that as L is increased, $g_H^{(K)}/g_{H,0}^{(K)}$ as a function of L and d_b, which is represented by $f(L,d_b)$ hereafter, first increases from unity and then decreases after passing through a maximum in the range of d_b investigated. Considering the asymptotic conditions $\lim_{L\to 0} f(L,d_b) = 1$ and $\lim_{L\to\infty} f(L, d_b) = \sqrt{3}/\left(2\sqrt{2}-1\right)$, which hold in the limit of $L/d_b \to \infty$, we have constructed an interpolation formula for $f(L,d_b)$, which may be written in the form,

$$\begin{aligned} f(L, d_b) &= 1 + a_1 L + a_2 L^2 \qquad \text{for } L < 6 \\ &= \left[b_0 - 1 + b_1(\ln\ L)^{-1}\right] \\ &\quad \times \exp\left[-b_2(\ln\ L)^{-1} - b_3(\ln\ L)^{-2}\right] + 1 \quad \text{for } L \geq 6. \end{aligned} \tag{35}$$

In Equation (35), the coefficients a_i ($i = 1, 2$) and b_i ($i = 0, 1, 2, 3$) may be given by

$$\begin{aligned} a_1 &= [f(6,d_b) - 3f'(6,d_b) - 1]/3 \\ a_2 &= [-f(6,d_b) + 6f'(6,d_b) + 1]/36 \end{aligned} \tag{36}$$

and

$$\begin{aligned} b_0 &= \sqrt{3}/\left(2\sqrt{2}-1\right) \\ b_1 &= 0.276181 + 0.473221 d_b - 0.240008 {d_b}^2 \\ &\quad + \left(0.018263 + 0.572154 {d_b}^2\right)\ln\ d_b \\ b_2 &= 2.66405 - 7.02277 d_b + 2.26380 {d_b}^2 \\ &\quad - \left(0.11568 + 7.14996 {d_b}^2\right)\ln\ d_b \\ b_3 &= 4.50327 + 0.06635 d_b + 4.03912 {d_b}^2 \\ &\quad + \left(0.33442 - 9.70377 {d_b}^2\right)\ln\ d_b, \end{aligned} \tag{37}$$

respectively, where $f'(L/d_b) = \partial f(L/d_b)/\partial L$. Note that in Equation (36) the values of $f(6,d_b)$ and $f'(6,d_b)$ may be calculated from Equation (35) and Equation (37). In Figure 4, the solid curves represent the values calculated from Equations (35)–(37) with the corresponding values of d_b. It is seen that the interpolation formula may well reproduce the numerical theoretical values in the ranges of L and d_b so examined, although for $0 \lesssim L \lesssim 1$ the numerical theoretical values seem to deviate downward slightly (up to 0.5%) from the corresponding values of the interpolation formula. Such a slight deviation is within experimental error (1% at least) in D determined by conventional methods and then causes no significant error in a practical use of the present interpolation formula for analysis of experimental data.

The factor $g_H^{(K)}(L,d_b)$ may therefore be approximately expressed as

$$g_H^{(K)}(L, d_b) = g_{H,0}^{(K)}(L/d_b) f(L, d_b), \tag{38}$$

where $g_{H,0}^{(K)}(L/d_b)$ and $f(L,d_b)$ are given by Equation (34) and Equation (35) with Equations (36) and (37), respectively. In Figure 1, the solid curves represent the approximate values calculated from Equation (38) with Equations (34)–(37) with the corresponding values of d_b. It is seen that the interpolation formula for $g_H^{(K)}(L,d_b)$ so proposed may well reproduce the numerical theoretical values in the ranges of d_b investigated and of $L/d_b \gtrsim 10$. The error in the value of $g_H^{(K)}$ in those ranges of d_b and L/d_b does not exceed 0.4%.

Comparison with experiment

Finally, we make a comparison of the present theoretical result with experimental data in a literature. Figure 5 shows plots of g_H against the logarithm of the weight-average molecular weight M_w for the regular three-arm star polystyrene in cyclohexane at 34.5 °C (Θ) obtained by Huber *et al.*[25] The open circles represent the experimental values. The curve represents the KP theory values of $g_H^{(K)}\left(\lambda\hat{L}, \lambda\hat{d}_b\right)$, where $\hat{L}$ and $\hat{d}_b$ is the total contour length and bead diameter, respectively, of the KP regular three-arm star touched-bead model in *real* length units, calculated from Equation (38) with Equations (34)–(37) along with the relation $\log M_w = \log \lambda\hat{L} + \log\left(\lambda^{-1} M_L\right)$ with M_L the molecular weight per unit contour length. The solid part of the curve indicates the range of $L/d_b \gtrsim 10$. The necessary KP parameter values used in the calculation of the KP theory values are $\lambda^{-1} = 20.0$ Å and $M_L = 39.0$ Å^{-1} determined by Norisuye and Fujita[26] for (linear) atactic polystyrene in cyclohexane at 34.5 °C (Θ) and $\hat{d}_b = 9.9$ Å estimated from the relation[27] $d = 0.891\hat{d}_b$ with d the hydrodynamic diameter of the KP cylinder model[8] using with $d = 8.8$ Å determined for the same system by Huber *et al.*[28] It is seen that the present theory may explain qualitatively the behavior of the experimental values, which increase with decreasing M_w, although including the range of $L/d_b \lesssim 10$.

CONCLUSION

We have evaluated the Kirkwood value $g_H^{(K)}$ and the KR one $g_H^{(KR)}$ of the ratio g_H of R_H of the unperturbed KP regular three-arm star touched-bead model to that of the KP linear one, both having the same (reduced) total contour length L and (reduced) bead diameter d_b. From an examination of the behavior of $g_H^{(K)}$ and that of $g_H^{(KR)}$ as functions of L and d_b, it is found that both of $g_H^{(K)}$ and $g_H^{(KR)}$ are insensitive to change in L irrespective of the value of d_b and that $g_H^{(KR)}$ is 3% at most larger than $g_H^{(K)}$ in the ranges of L and d_b. The empirical interpolation formula for $g_H^{(K)}$ has been constructed, which reproduces the asymptotic values $\sqrt{3}/(2\sqrt{2}-1)$ $(=0.947)$ in the random-coil limit and 1 in the thin-rod limit.

CONFLICT OF INTEREST

The author declares no conflict of interest.

1 Ida, D. & Yoshizaki, T. A Monte Carlo study of the intrinsic viscosity of semiflexible regular three-arm star polymers. *Polym. J.* **39**, 1373–1382 (2007).
2 Ida, D., Nakamura, Y. & Yoshizaki, T. Intrinsic viscosity of wormlike regular three-arm stars. *Polym. J.* **40**, 256–267 (2008).
3 Ida, D. & Yoshizaki, T. A Monte Carlo study of the second virial coefficient of semiflexible regular three-arm star polymers. *Polym. J.* **40**, 1074–1080 (2008).
4 Mansfield, M. L. & Stockmayer, W. H. Unperturbed dimensions of wormlike stars. *Macromolecules* **13**, 1713–1715 (1980).
5 Kirkwood, J. G. The statistical mechanical theory of irreversible processes in solutions of flexible macromolecules. Visco-elastic behavior. *Rec. Trav. Chim.* **68**, 649–660 (1949).
6 Kirkwood, J. G. The general theory of irreversible processes in solutions of macromolecules. *J. Polym. Sci.* **12**, 1–14 (1954).
7 Yamakawa, H. *Modern Theory of Polymer Solutions* (Harper & Row, New York, NY, USA, 1971). Its electronic edition is available online at the URL http://www.molsci.polym.kyoto-u.ac.jp/archives/redbook.pdf.
8 Yamakawa, H. *Helical Wormlike Chains in Polymer Solutions* (Springer, Berlin, 1997).
9 Yamada, T., Yoshizaki, T. & Yamakawa, H. Transport coefficients of helical wormlike chains. 5. Translational diffusion coefficient of the touched-bead model and its application to oligo- and polystyrenes. *Macromolecules* **25**, 377–383 (1992).
10 Kirkwood, J. G. & Riseman, J. The intrinsic viscosities and diffusion constants of flexible macromolecules in solution. *J. Chem. Phys.* **16**, 565–573 (1948).
11 Kurata, M. & Yamakawa, H. Theory of dilute polymer solution. II. Osmotic pressure and frictional properties. *J. Chem. Phys.* **29**, 311–325 (1958).
12 Zimm, B. H. Dynamics of polymer molecules in dilute solution: viscoelasticity, flow birefringence and dielectric loss. *J. Chem. Phys.* **24**, 269–278 (1956).
13 Yamakawa, H. & Yoshizaki, T. Dynamics of helical wormlike chains. I. Dynamic model and diffusion equation. *J. Chem. Phys.* **75**, 1016–1030 (1981).
14 Yamakawa, H. & Yoshizaki, T. Dynamics of helical wormlike chains. XI. Translational diffusion with fluctuating hydrodynamic interaction. *J. Chem. Phys.* **91**, 7900–7911 (1989).
15 Kurata, M. & Fukatsu, M. Unperturbed dimension and translational friction constant of branched polymers. *J. Chem. Phys.* **41**, 2934–2944 (1964).
16 Stockmayer, W. H. & Fixman, M. Dilute solutions of branched polymers. *Ann. NY. Acad. Sci.* **57**, 334–352 (1953).
17 Irurzun, I. M. Hydrodynamic properties of regular star-branched polymer in dilute solution. *J. Polym. Sci. B Polym. Phys.* **35**, 563–567 (1997).
18 Zimm, B. H. & Stockmayer, W. H. The dimensions of chain molecules containing branches and rings. *J. Chem. Phys.* **17**, 1301–1314 (1949).
19 Riseman, J. & Kirkwood, J. G. The intrinsic viscosity, translational and rotatory diffusion constants of rod-like macromolecules in solution. *J. Chem. Phys.* **18**, 512–516 (1950).
20 Tchen, C.-M. Motion of small particles in skew shape suspended in a viscous liquid. *J. Appl. Phys.* **25**, 463–473 (1954).
21 Zwanzig, R. Translational diffusion in polymer solutions. *J. Chem. Phys.* **45**, 1858–1859 (1966).
22 Paul, E. & Mazo, R. M. Translational diffusion coefficient of a plane polygonal polymer. *J. Chem. Phys.* **48**, 2378–2378 (1968).
23 Paul, E. & Mazo, R. M. Hydrodynamic properties of a plane-polygonal polymer. According to Kirkwood-Riseman theory. *J. Chem. Phys.* **51**, 1102–1107 (1969).
24 Yamakawa, H. & Yamaki, J. Translational diffusion coefficients of plane-polygonal polymers: application of the modified Oseen tensor. *J. Chem. Phys.* **57**, 1542–1546 (1972).
25 Huber, K., Burchard, W. & Fetters, L. J. Dynamic light scattering of regular star-branched molecules. *Macromolecules* **17**, 541–548 (1984).
26 Norisuye, T. & Fujita, H. Excluded-volume effects in dilute polymer solutions. XIII. Effects of chain stiffness. *Polym. J.* **14**, 143–147 (1982).
27 Yamakawa, H. Some remarks on the transport theory for wormlike cylinder models. *Macromolecules* **16**, 1928–1931 (1983).
28 Huber, K., Bantle, S., Lutz, P. & Burchard, W. Hydrodynamic and thermodynamic behavior of short-chain polystyrene in toluene and cyclohexane at 34.5°C. *Macromolecules* **18**, 1461–1467 (1985).

APPENDIX

Asymptotic form for *D* of the regular three-arm star in the rod limit

In this appendix, we derive the asymptotic solutions in the limit of $L/d_b \to \infty$ (thin- or long-rod limit) for $D^{(K)}$ and $D^{(KR)}$ of the KP regular three-arm star in the rod limit.

Kirkwood value

The asymptotic form of $D^{(K)}$ for the regular three-arm star in the thin-rod limit may be directly derived from Equation (4) with Equations (5)–(7) and (15).

In the case of the regular three-arm star, the summation in Equation (4) may be rewritten in the form,

$$\sum_{\substack{i=0\\ i\neq j}}^{n}\sum_{j=0}^{n}\left\langle R_{ij}^{-1}\right\rangle = 2\left[\sum_{i=0}^{2}\sum_{j=1}^{m}\left\langle {R_{0(im+j)}}^{-1}\right\rangle + \sum_{i=0}^{2}\sum_{j=1}^{m-1}\sum_{k=j+1}^{m}\left\langle {R_{(im+j)(im+k)}}^{-1}\right\rangle + \sum_{i=0}^{1}\sum_{j=i+1}^{2}\sum_{k=1}^{m}\sum_{l=1}^{m}\left\langle {R_{(im+k)(jm+l)}}^{-1}\right\rangle\right]. \quad (39)$$

Recall that $L=(n+1)d_b$ and $m=n/3$. In the limit of $L/d_b \to \infty$, that is, $m \to \infty$, we may perform the first and second summations on the right-hand side of Equation (39) as follows:

$$\sum_{i=0}^{2}\sum_{j=1}^{m}\left\langle {R_{0(im+j)}}^{-1}\right\rangle = \frac{3}{d_b}\left[\ln\ m + \gamma_E + \mathcal{O}\left(m^{-1}\right)\right],$$
$$\sum_{i=0}^{2}\sum_{j=1}^{m-1}\sum_{k=j+1}^{m}\left\langle {R_{(im+j)(im+k)}}^{-1}\right\rangle = \frac{3m}{d_b}\left[\ln\ m + \gamma_E - 1 + \mathcal{O}\left(m^{-1}\right)\right], \quad (40)$$

where γ_E $(=0.5772\cdots)$ is the Euler constant. In this limit, the third summation on the right-hand side of Equation (39) may be converted to an integral and it may be calculated to be

$$\sum_{i=0}^{1}\sum_{j=i+1}^{2}\sum_{k=1}^{m}\sum_{l=1}^{m}\left\langle {R_{(im+k)(jm+l)}}^{-1}\right\rangle = \frac{3m}{d_b}\left[\ln\left(3+2\sqrt{3}\right) - 3(\ln\ 3)/2 - \ln\left(2-\sqrt{3}\right)\right]. \quad (41)$$

Then we have

$$\lim_{\substack{L\to 0\\ L/d_b\to\infty}}\sum_{\substack{i=0\\ i\neq j}}^{n}\sum_{j=0}^{n}\left\langle R_{ij}^{-1}\right\rangle = \frac{2L}{d_b^2}\left[\ln(L/d_b) + \mathcal{O}\left(\left[\ln(L/d_b)\right]^0\right)\right]. \quad (42)$$

From Equation (4) and Equation (42), we obtain Equation (26).

KR value

In the thin-rod limit, we may convert the summations in Equations (16) and (17) to integrals. In the case of the regular three-arm star, Equation (16) with Equation (17) may then be rewritten

in the form,

$$D^{(\mathrm{KR})} = k_{\mathrm{B}}T\left[3\pi\eta_0 L\int_0^1 \psi(x)dx\right]^{-1}, \tag{43}$$

where $\psi(x)$ is the solution of the integral equation,

$$\psi(x) = 1 - \frac{1}{2}\left[\int_0^1 K_0(x,t)\psi(t)dt + 2\int_0^1 K_1(x,t)\psi(t)dt\right]. \tag{44}$$

In Equation (44), $K_0(x,t)$ and $K_1(x,t)$ are the continuous versions of the mean reciprocal of the distance between the centers of two beads on the same arm and on the different arm, respectively, and they are explicitly given by

$$\begin{aligned} K_0(x,t) &= |x-t|^{-1} \quad \text{for} \quad |x-t| \geq 3d_{\mathrm{b}}/L \\ &= 0 \qquad\quad\ \ \text{for} \quad |x-t| < 3d_{\mathrm{b}}/L, \end{aligned} \tag{45}$$

$$K_1(x,t) = \left(x^2 + t^2 + xt\right)^{-1/2}. \tag{46}$$

From Equation (44), the function $F(x)$ may be defined by

$$\begin{aligned} F(x) &= 1 - 2\phi(x) \\ &= \int_0^1 K_0(x,t)\phi(t)\,\mathrm{d}t + 2\int_0^1 K_1(x,t)\phi(t)\,\mathrm{d}t, \end{aligned} \tag{47}$$

where $\phi(x) = \psi(x)/2$. We then expand $\phi(x)$ and $K_k(x,t)$ $(k = 0,\ 1)$ in terms of the shifted Legendre polynomial $\tilde{P}_l(x)$ as follows:

$$\phi(x) = \sum_{i=0}^{\infty} \phi_i \tilde{P}_i(x), \tag{48}$$

$$K_k(x,t) = \sum_{i=0}^{\infty}\sum_{j=0}^{\infty} K_{k,ij}\tilde{P}_i(x)\tilde{P}_j(t) \quad (k = 0, 1), \tag{49}$$

where $\tilde{P}_l(x)$ is defined by

$$\tilde{P}_l(x) = (-1)^l P_l(2x-1) \tag{50}$$

with $P_l(x)$ the Legendre polynomial. We note that $\tilde{P}_l(x)$ satisfies the following orthogonality relation,

$$\int_0^1 \tilde{P}_l(x)\tilde{P}_{l'}(x)\,\mathrm{d}x = (2l+1)^{-1}\delta_{ll'}, \tag{51}$$

where $\delta_{ll'}$ is the Kronecker delta. In Equations (48) and (49), the expansion coefficients ϕ_i and $K_{k,ij}$ may be given by

$$\phi_i = (2i+1)\int_0^1 \phi(x)\tilde{P}_i(x)\,\mathrm{d}x \tag{52}$$

and

$$K_{k,ij} = (2i+1)(2j+1)\int_0^1\int_0^1 K_k(x,t)\tilde{P}_i(x)\tilde{P}_j(t)\,\mathrm{d}x\,\mathrm{d}t \quad (k = 0, 1), \tag{53}$$

respectively. Substituting Equations (52) and (53) into the second line of Equation (47) and carrying out the integrations, $F(x)$ may be rewritten in the form,

$$F(x) = \sum_{i=0}^{\infty}\sum_{j=0}^{\infty}(2j+1)^{-1}\left(K_{0,ij} + 2K_{1,ij}\right)\phi_j\tilde{P}_i(x). \tag{54}$$

It can be shown in the limit of $L/d_{\mathrm{b}} \to \infty$ that

$$K_{0,ij} = (-1)^{i+j}(4j+2)\delta_{ij}\ln(L/d_{\mathrm{b}}) + \mathcal{O}\left([\ln(L/d_{\mathrm{b}})]^0\right) \tag{55}$$

and $K_{1,ij} = \mathcal{O}\left([\ln(L/d_{\mathrm{b}})]^0\right)$. Then we have

$$F(x) = \left[2\ln(L/d_{\mathrm{b}}) + \mathcal{O}\left([\ln(L/d_{\mathrm{b}})]^0\right)\right]\phi(x). \tag{56}$$

From the first line of Equation (47) and Equation (56) along with the relation $\varphi(x) = \psi(x)/2$, $\psi(x)$ may be written in the from,

$$\psi(x) = \left[\ln(L/d_{\mathrm{b}}) + \mathcal{O}\left([\ln(L/d_{\mathrm{b}})]^0\right)\right]^{-1}. \tag{57}$$

Substituting of Equation (57) into Equation (43) and carrying out the integration over x, we obtain Equation (30).